

COMMUNICATION

Fish and chips: implementation of a neural network model into computer chips to maximize swimming efficiency in autonomous underwater vehicles

R W Blake¹, H Ng², K H S Chan¹ and J Li¹

¹ Department of Zoology, University of British Columbia, British Columbia, V6T 1Z4, Canada

² Information Technology, University of British Columbia, British Columbia, V6T 1Z2, Canada

E-mail: blake@zoology.ubc.ca, omega.centari@hotmail.com, chankhs@zoology.ubc.ca,
lijason@zoology.ubc.ca

Received 28 April 2008

Accepted for publication 13 June 2008

Published 15 July 2008

Online at stacks.iop.org/BB/3/034002

Abstract

Recent developments in the design and propulsion of biomimetic autonomous underwater vehicles (AUVs) have focused on boxfish as models (e.g. Deng and Avadhanula 2005). Biomimetic micro underwater vehicle with oscillating fin propulsion: system design and force measurement *Proc. 2005 IEEE Int. Conf. Robot. Auto. (Barcelona, Spain)* pp 3312–7). Whilst such vehicles have many potential advantages in operating in complex environments (e.g. high manoeuvrability and stability), limited battery life and payload capacity are likely functional disadvantages. Boxfish employ undulatory median and paired fins during routine swimming which are characterized by high hydromechanical Froude efficiencies (≈ 0.9) at low forward speeds. Current boxfish-inspired vehicles are propelled by a low aspect ratio, 'plate-like' caudal fin (ostraciiform tail) which can be shown to operate at a relatively low maximum Froude efficiency (≈ 0.5) and is mainly employed as a rudder for steering and in rapid swimming bouts (e.g. escape responses). Given this and the fact that bioinspired engineering designs are not obligated to wholly duplicate a biological model, computer chips were developed using a multilayer perception neural network model of undulatory fin propulsion in the knifefish *Xenomystus nigri* that would potentially allow an AUV to achieve high optimum values of propulsive efficiency at any given forward velocity, giving a minimum energy drain on the battery. We envisage that externally monitored information on flow velocity (sensory system) would be conveyed to the chips residing in the vehicle's control unit, which in turn would signal the locomotor unit to adopt kinematics (e.g. fin frequency, amplitude) associated with optimal propulsion efficiency. Power savings could protract vehicle operational life and/or provide more power to other functions (e.g. communications).

(Some figures in this article are in colour only in the electronic version)

1. Introduction

Much research and development on autonomous underwater vehicles (AUVs) has focused on larger vehicles driven by

propellers (Bandyopadhyay 2004) or undulatory body motions (Triantafyllou and Triantafyllou 1995, Ostrowski and Burdick 1998, Triantafyllou *et al* 2000, Morgansen *et al* 2001, Kim and Youm 2004). More recently, developments in unsteady

fluid dynamics and biomimetic microtechnology have lent themselves to the fabrication of centimetre scale microrobots' micro-underwater vehicles (MUVs) based on boxfish models (Deng and Avadhanula 2005). Like boxfish, such MUVs would be effective in complex environments requiring slower swimming speeds and high manoeuvrability and stability. Whilst swimming mechanics in boxfish is well understood (e.g. routine swimming performance, manoeuvrability and stability, carapace hydrodynamics (drag and lift, vortical flow self-correcting forces); Walker 2000, Gordon *et al* 2000, Hove *et al* 2001, Blake 2004, Bartol *et al* 2008), little attention has been given to MUV functional design and operation. Deng and Avadhanula (2005) present a biomimetic system concept design, fabrication details and experimental force measurements on prototype boxfish-inspired MUVs. A central processing unit (CPU) sends a control signal to the locomotor unit which in turn receives energy from a power supply (battery) feeding back to the CPU. Possible functional disadvantages of MUVs are limited payload capacity and battery life.

Here, we develop control unit computer chips designed to optimize propulsive efficiency relative to flow velocity. External information on flow (sensory system) could send sensor signals to the CPU that in turn would send a control signal to the locomotory unit allowing actuators to operate at maximum efficiency relative to perceived flow conditions saving battery power that could protract vehicle life, allow for a larger payload or provide additional power for other functions (e.g. communications).

2. Methods

We developed three computer chips based on multilayer perception neural network models (Li *et al* 2007) of the hydrodynamic efficiencies of swimming in the knifefish *Xenomystus nigri* Günther. Specifically, a neural network model was implemented into computer chips by (1) construction of networks with the optimal topology based on experimental data; (2) sensitivity analysis of determinant factors for the Froude efficiency η_p (forward velocity U , fin lateral velocity $W = \partial h / \partial t$ where h is the distance displaced by the fin's trailing edge, lateral velocity of pushing on the water $w = (\partial h \partial t^{-1}) + U(\partial h \partial x^{-1})$); (3) validation and testing of network predictions and (4) implementation of the neural network into three computer chips.

Neural networks are characterized by distinct topologies of nonlinear differentiable activation functions in neurons consisting of input, output and hidden layers such that each neuron of a layer is connected to all others in the next (McCulloch and Pitts 1943). Following Li *et al* (2007), the optimal neural network configuration was adopted from a neighbourhood of 1–3 layers of 1–10 neurons. We used the momentum learning method, an advanced adaptive patterning learning technique progressed from the classic gradient descent method (Salehfar and Benson 1998). Gradient descent incorporates error back propagation algorithm to train weights (based on local information) for minimizing overall error. The instantaneous error of neuron i at the n th training iteration is

$$e_i(n) = d_i(n) - y_i(n), \quad (1)$$

where $e_i(n)$ is the instantaneous error, $d_i(n)$ is the desired output and $y_i(n)$ is the neuron output (Kong *et al* 1998). Weights are trained from the iteration $n + 1$ in gradient descent:

$$W_{ij}(n + 1) = W_{ij}(n) + \gamma \delta_i(n) x_j(n), \quad (2)$$

where $W_{ij}(n)$ is the weight between nodes i and j at iteration n , x_j is the present input, $\delta_i(n)$ is the local gradient which pointed to the required change in the weight and γ is the learning rate. This method was improved by incorporating 'momentum learning' to decrease noise and increase convergence:

$$\hat{W}_{ij}(n + 1) = W_{ij}(n + 1) + \alpha (W_{ij}(n) - W_{ij}(n - 1)), \quad (3)$$

where $\hat{W}_{ij}(n + 1)$ and $W_{ij}(n)$ are the weights between nodes i and j at iteration n for momentum learning and gradient descent respectively and α is the momentum factor. The stopping criterion was chosen at maximum epoch (iterations through the patterns represented in the input) of 1000 and at a mean square error (MSE) ≤ 0.01 :

$$\text{MSE} = \frac{\sum_{j=0}^p \sum_{i=0}^m (d_{ij} - y_{ij})^2}{m \cdot p}, \quad (4)$$

where m is the size of the training dataset, p is the total number of neurons and y_{ij} and d_{ij} are the network and desired output for data series i at neuron j respectively.

Input data for analysis of the fin motions of *X. nigri* are derived from a simplified bulk momentum approach based on elongated body theory (Lighthill 1969), where the mean thrust power \bar{P} is given by subtracting the mean rate at which kinetic energy is wasted in the wake \bar{P}_k from the total mean rate of working \bar{P}_t :

$$\bar{P} = \bar{P}_t - \bar{P}_k = U(\overline{MwW}) - 0.5U(\overline{Mw^2}), \quad (5)$$

where M is the added mass at the trailing edge of the undulatory anal fin ($M = \frac{1}{4}\pi\rho d_s^2\beta$, where ρ , d_s and β are water density, the depth of a propulsive section and shape factor respectively ($\beta \approx 1$; Lighthill 1970)). The propulsive efficiency η_p is

$$\eta_p = 1 - (\bar{P}_t - \bar{P}) / \bar{P}_t. \quad (6)$$

The values for W , w , \bar{P} , \bar{P}_t , \bar{P}_k and η_p as a function of the swimming velocity U were taken from Blake (1983; table 1).

Sensitivity analysis was performed on the trained neural network to determine the relative importance of each variable using weights derived from the training process and measuring the change in the predicted output for every 50 divisions of 1 SD of the mean input (Masters 1993, Dollhopf *et al* 2004). The optimality and accuracy was tested based on the cross-validation scheme using 50% of the dataset for training and 50% for MLP-NN performance testing. The sensitivity analysis showed that the swimming speed U and fin lateral speed W were the major determinants of η_p for implementation into computer chips (figure 1(A)). The neural network model was then constructed based on the cross-validation scheme (75% of the data were used to train the neural network and 25% was used to test its performance) and good agreement was found between neural network predictions and actual values ($P > 0.05$). Figure 1(B) shows a 3D representation of the output from the trained neural network based on U , W and η_p .

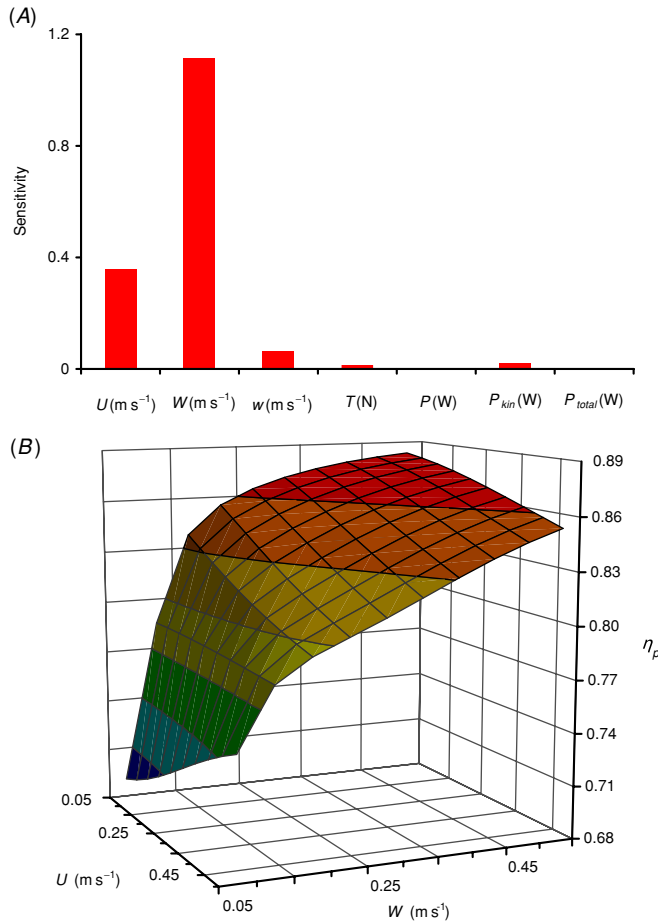


Figure 1. (A) Sensitivity for the predicted efficiency η_p (defined as the change in the mean output for every 50 divisions within 1 SD of the mean input), swimming speed U , lateral velocity of the fin W , lateral velocity of pushing on the water slice w , thrust T , mean thrust power P , kinetic energy wasted in the wake P_{kin} and mean total power P_{tot} . (B) Three-dimensional plot of the predicted output η_p as a function of the lateral velocity of the fin W and swimming speed U . (This figure is in colour only in the electronic version)

Three computer chip designs were constructed: (1) fin lateral speed versus swimming speed giving propulsive efficiency (figure 2), (2) propulsive efficiency versus fin lateral speed giving swimming speed (figure 3) and (3) propulsive efficiency versus swimming speed giving fin lateral speed (figure 4). The implementation of figures 2–4 consist of 1918, 2318 and 2362 integrated circuits (ICs) respectively and multiple modules with two, three and four 6-bit inputs controlling each module of chips (gates 1, 2 and 3 respectively). Each module is interconnected via a matrix design and activated by two input controls. The circuit is initiated when the two inputs are entered.

Each circuit represents an entire array of swimming efficiencies, swim speeds and fin speed efficiencies. Multiple, redundant outputs are combined into one output via the merger (figure 5) to reduce the number of connections required to display the final results. Figure 5 shows that an individual output connection state is either enabled or disabled and that the circuit is forward feeding (i.e. current flow does not oppose

the input direction). The flow is always on high and buffered inverters negate the current flow to low. The matrix is run in parallel where voltage is either high or low on all the interconnected circuits and the computations within the matrix and outputs representing the control signals are all digital. Circuit architecture is based on several different configurations of the gates (figure 5) and each can determine the output efficiency.

Bus sizes of 12 and 13 bits were constructed for the computer chips based on Boolean logic functions. The outputs for the first computer chip (figure 2) of gates 1 η_p (gate 1), 2 η_p (gate 2) and 3 η_p (gate 3) are

$$\eta_p(\text{gate 1}) = (A_0 \wedge B_0) \wedge (A_1 \wedge B_1) \wedge (A_2 \wedge B_2) \wedge (A_3 \wedge B_3) \wedge (A_4 \wedge B_4) \wedge (A_5 \wedge B_5) \quad (7)$$

$$\eta_p(\text{gate 2}) = \{(A_0 \wedge B_0) \wedge (A_1 \wedge B_1) \wedge (A_2 \wedge B_2) \wedge (A_3 \wedge B_3) \wedge (A_4 \wedge B_4) \wedge (A_5 \wedge B_5)\} \vee \{(A_0 \wedge C_0) \wedge (A_1 \wedge C_1) \wedge (A_2 \wedge C_2) \wedge (A_3 \wedge C_3) \wedge (A_4 \wedge C_4) \wedge (A_5 \wedge C_5)\} \quad (8)$$

and

$$\eta_p(\text{gate 3}) = \{(A_0 \wedge B_0) \wedge (A_1 \wedge B_1) \wedge (A_2 \wedge B_2) \wedge (A_3 \wedge B_3) \wedge (A_4 \wedge B_4) \wedge (A_5 \wedge B_5)\} \vee \{(A_0 \wedge C_0) \wedge (A_1 \wedge C_1) \wedge (A_2 \wedge C_2) \wedge (A_3 \wedge C_3) \wedge (A_4 \wedge C_4) \wedge (A_5 \wedge C_5)\} \vee \{(A_0 \wedge D_0) \wedge (A_1 \wedge D_1) \wedge (A_2 \wedge D_2) \wedge (A_3 \wedge D_3) \wedge (A_4 \wedge D_4) \wedge (A_5 \wedge D_5)\} \quad (9)$$

respectively where $A_0, A_1, A_2, A_3, A_4, A_5, B_0, B_1, B_2, B_3, B_4, B_5, C_0, C_1, C_2, C_3, C_4, C_5, D_0, D_1, D_2, D_3, D_4$ and D_5 are each 1 bit and can be negated (\neg) and the two switches are $A_0 \wedge A_1 \wedge A_2 \wedge A_3 \wedge A_4 \wedge A_5$ and $B_0 \wedge B_1 \wedge B_2 \wedge B_3 \wedge B_4 \wedge B_5$ for fin lateral speed and swimming speed respectively. Outputs for the second and third computer chips (figures 3 and 4) of gates 1 $\eta_{q,r}$ (gate 1) and 2 $\eta_{q,r}$ (gate 2) are

$$\eta_{q,r}(\text{gate 1}) = ((A_0 \wedge B_0) \wedge (A_1 \wedge B_1) \wedge (A_2 \wedge B_2) \wedge (A_3 \wedge B_3) \wedge (A_4 \wedge B_4) \wedge (A_5 \wedge B_5)) \wedge A_6 \quad (10)$$

and

$$\eta_{q,r}(\text{gate 2}) = \left\{ ((A_0 \wedge B_0) \wedge (A_1 \wedge B_1) \wedge (A_2 \wedge B_2) \wedge (A_3 \wedge B_3) \wedge (A_4 \wedge B_4) \wedge (A_5 \wedge B_5)) \wedge A_6 \right\} \vee \left\{ ((A_0 \wedge C_0) \wedge (A_1 \wedge C_1) \wedge (A_2 \wedge C_2) \wedge (A_3 \wedge C_3) \wedge (A_4 \wedge C_4) \wedge (A_5 \wedge C_5)) \wedge A_6 \right\} \quad (11)$$

respectively where the variables are each 1 bit and can be negated. The two switches are $A_0 \wedge A_1 \wedge A_2 \wedge A_3 \wedge A_4 \wedge A_5 \wedge A_6$ and $B_0 \wedge B_1 \wedge B_2 \wedge B_3 \wedge B_4 \wedge B_5$.

3. Results and discussion

Figures 2–4 show the implemented schematic diagram of the computer chips that output the optimum swimming efficiency, swim speed and fin lateral speed respectively. The high quality of the computer chips is demonstrated in their outputs

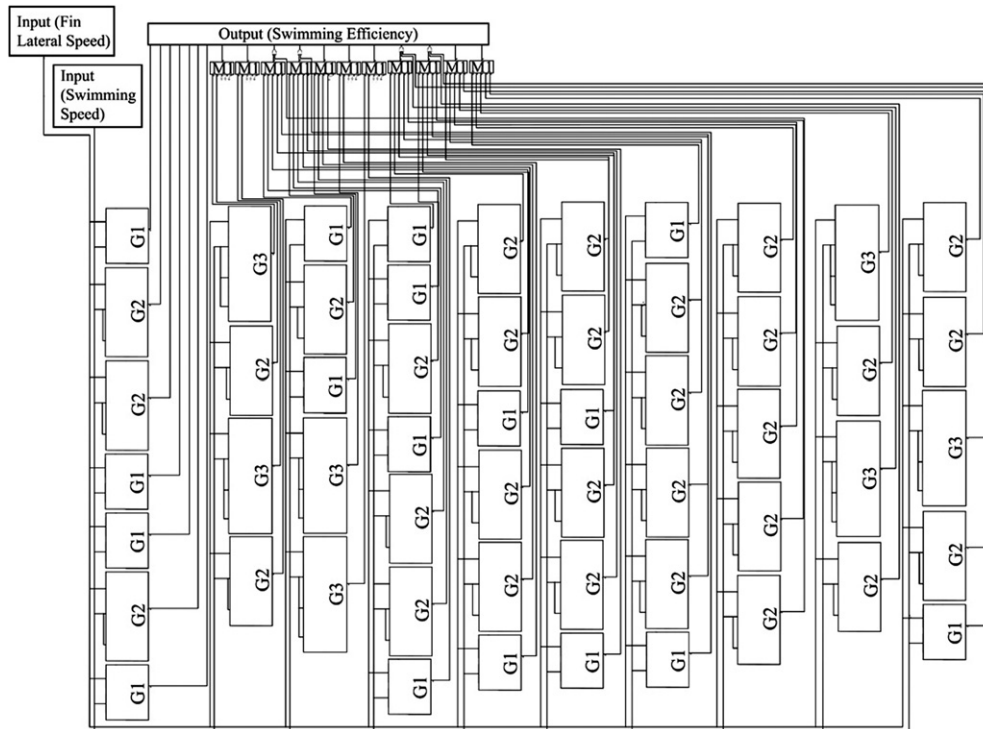


Figure 2. Computer chip for the propulsive efficiency η_p as a function of the fin lateral speed W versus swimming speed U . Multiple (1918 in total) integrated circuits are implemented in modules (gates 1, 2 and 3, with two, three and four 6-bit inputs, respectively) interconnected via a matrix design. Multiple, redundant outputs are combined into one output via the merger M1 (figure 5).

which are all equal to the neural network model. This supports the proposition of incorporating them into the CPU of AUVs. Figure 1(A) shows that the neural network model is most sensitive to the fin lateral velocity W and the forward velocity U . The values of propulsive efficiency exceed 0.7 and asymptote at about 0.9 at higher forward velocities.

Deng and Avadhanula (2005) give a basic design overview and ‘simulator architecture’ for the major design units of biomimetic MUVs based on oscillatory propulsion employing a boxfish model. There are five main units: locomotory, sensory, power, communications and control. Whilst the nature of the propulsion system may vary depending on the biomimetic model (boxfish (e.g. Deng and Avadhanula 2005), anguilliform (e.g. Ostrowski and Burdick 1998), carangiform (e.g. Morgansen *et al* 2001), thunniform (e.g. Triantafyllou and Triantafyllou 1995) and undulatory fin model (Collins *et al* 2008)), the basic design overview presented by Deng and Avadhanula (2005) is generally applicable. Deng and Avadhanula’s (2005) MUV is propelled by an electromechanical actuated-fin system. Two side fins (for steering and moving upward and downward) and a plate-like caudal fin (ostraciiform tail) for propulsion are driven by a PZT bimorph actuator with motion amplification from four bar mechanisms. The fins are powered by electric energy (e.g. lithium battery) and the power supply, communications (e.g. ultrasonic transmitters), sensory (e.g. flow velocity detection) units feed into the control (CPU) unit.

We envisage that part of a control unit could contain the three chips necessary to optimize propulsive efficiency relative to the flow velocity. External information on flow velocity

could be conveyed by sensor signals to the control unit which in turn could instruct the locomotor unit (say an undulatory fin) to appropriately match fin frequency, and hence W , to achieve optimum propulsive efficiency. Under these conditions, the energy drain on the power unit will be a minimum at any given U . This power saving could protract the operational life of the vehicle and/or provide more power to non-locomotor functions (e.g. sensors, communications).

Currently, the ‘ostraciiform model’ is favoured with respect to the design and function of small, highly manoeuvrable and stable AUVs (e.g. Gordon *et al* (2000), Bartol *et al* (2003), Blake (2004), Deng and Avadhanula (2005)). Whilst this approach to AUV function is appropriate and promising as far as body design, manoeuvrability and stability are concerned, the current focus on an oscillating plate as a basis for propulsion might be given further consideration. In particular, it can be shown that the maximum Froude efficiency of a low aspect ratio ‘plate-like’ caudal fin propeller (ostraciiform tail) has a relatively low upper value (≈ 0.5 ; M J Lighthill in Blake (1981)). In fact, boxfish are not propelled by the reciprocating motions of their caudal fin during routine activity. Rather, they swim through the action of undulatory median and paired fins and, in rectilinear swimming, the caudal fin is often collapsed presumably to reduce drag (Blake 1977). The caudal fin is mainly employed as a rudder for steering and in bouts of unsteady swimming (R W Blake, unpublished observations).

Undulatory median and paired fin swimming is an adaptation for propulsion for high hydromechanical efficiency at low forward speeds (Blake 2004). Given that

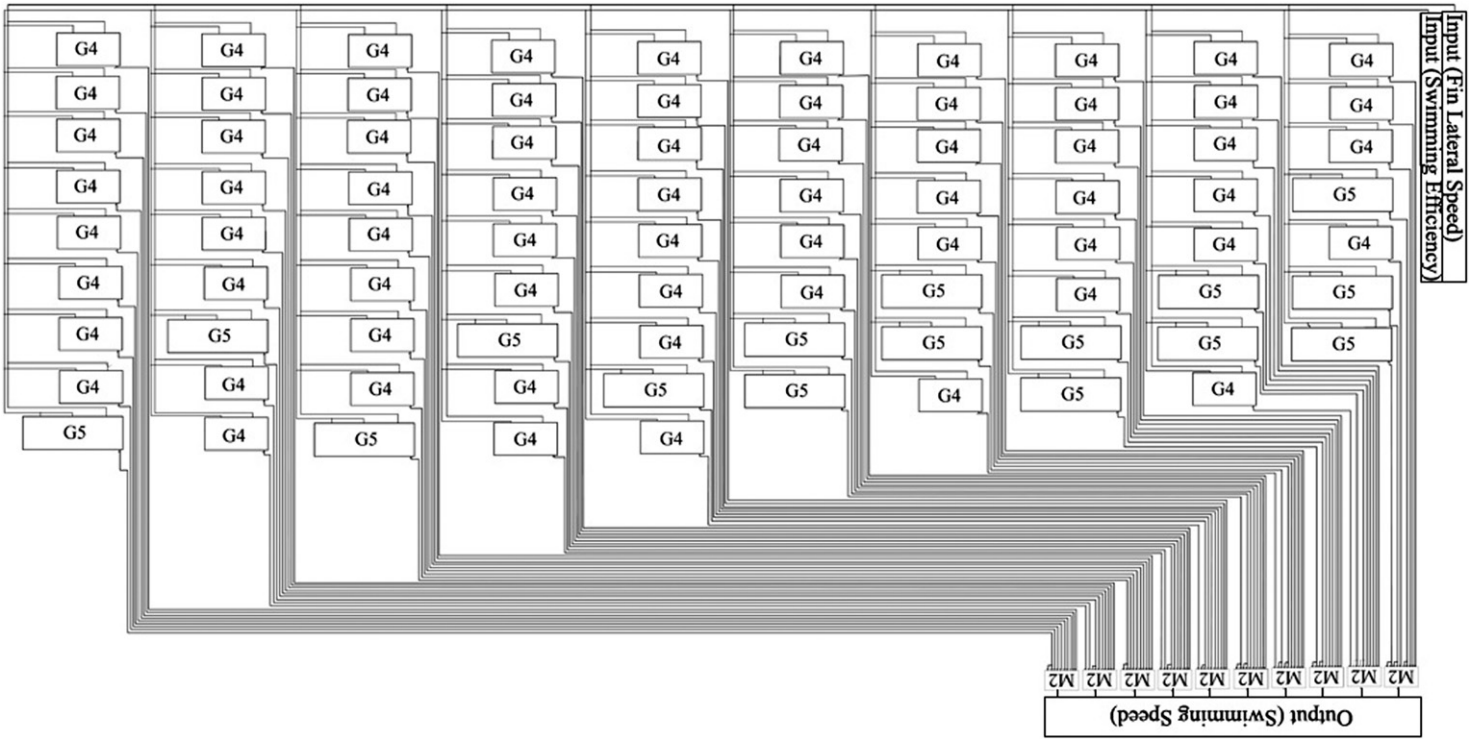


Figure 3. Computer chip for the swimming speed U as a function of the efficiency η_p and fin lateral speed W . Multiple (2318) integrated circuits are implemented in modules (gates 4 and 5, with two and three 6-bit inputs, respectively) interconnected via a matrix design. Multiple, redundant outputs are combined into one output via the merger M2 (figure 5).

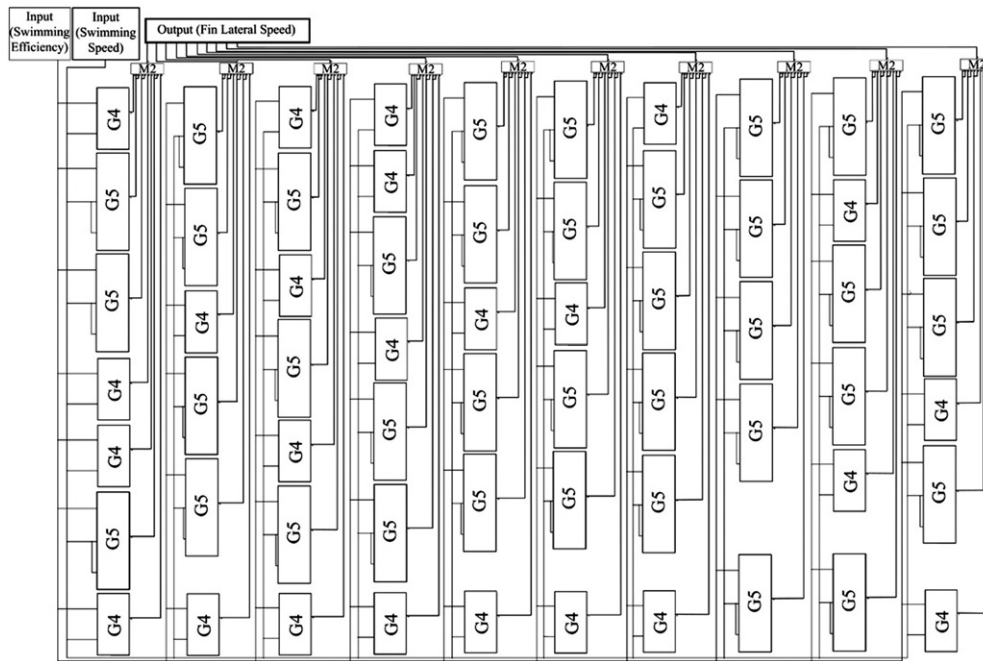


Figure 4. Computer chip for the fin lateral speed W as a function of the efficiency η_p and swimming speed U . Multiple (2362) integrated circuits are implemented in modules (gates 4 and 5, with two and three 6-bit inputs, respectively) interconnected via a matrix design. Multiple, redundant outputs are combined into one output via the merger M2 (figure 5).

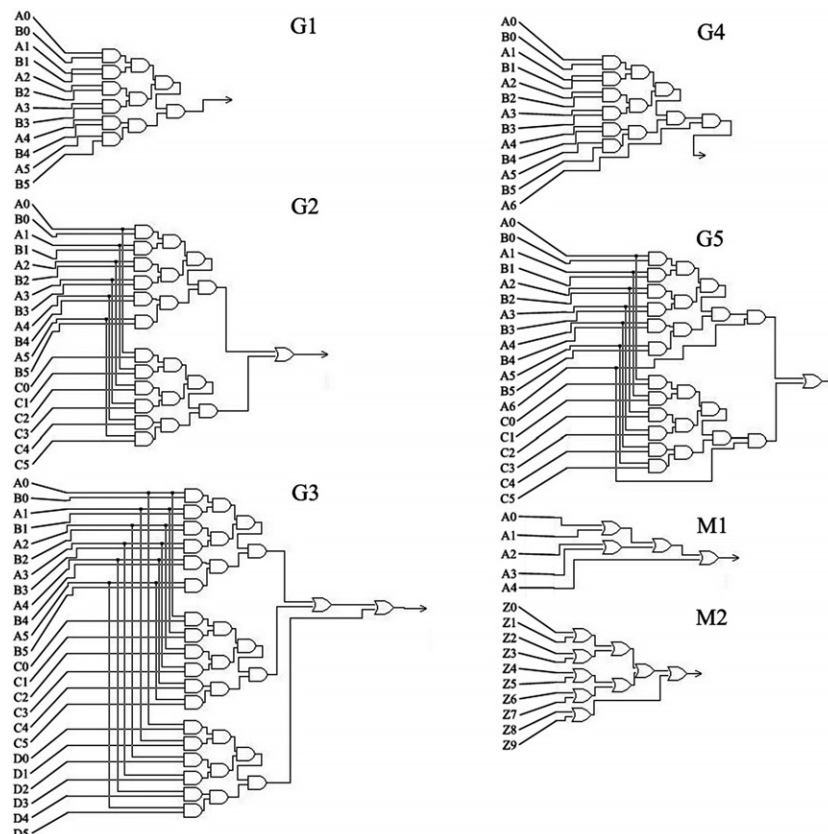


Figure 5. Circuit architecture is based on several different configurations of the gates (gates 1, 2, 3, 4 and 5, with two, three, four, two and three 6-bit inputs, respectively) and mergers M1 and M2 to combine multiple outputs into one output.

biomimetically inspired engineering designs need not be constrained by the limitations imposed by phylogenetic (historical) or ontogenetic (developmental) factors, optimal

structural and functional solutions can be found by selecting appropriate design features from a variety of ‘fish models’. Specifically, Deng and Avadhanula’s (2005) boxfish-based

MUV could combine the relatively low drag, high stability and manoeuvrability given by the boxfish carapace body form (Bartol *et al* 2008) with an undulatory fin-based propulsion system rather than the current oscillating fin design. Biomimetic undulatory fins have been developed (sinusoidally undulating flexible fins with distributed compliance based on a rib structure; Trease *et al* 2003). This material design has recently been incorporated into a 'WaveDrive' actuating mechanism and preliminary measurements have been made on thrust production (Collins *et al* 2008).

Further research on the performance of a prototype AUV combining a boxfish-inspired form (e.g. Deng and Avadhanula (2005)) equipped with flow sensors, an undulatory fin actuator (e.g. Trease *et al* (2003), Collins *et al* (2008)) and a simulator architecture with a CPU incorporating the computer chips described here is warranted.

Acknowledgments

RWB thanks the Natural and Science Engineering Research of Canada for financial support. KHSC is funded by Graduate Entrance and McLean Fraser Memorial Scholarships (UBC).

References

- Bandyopadhyay P R 2004 Trends in biorobotic autonomous undersea vehicles *IEEE J. Ocean. Eng.* **29** 109–39
- Bartol I K, Gharib M, Weihs D, Webb P W, Hove J R and Gordon M S 2003 Hydrodynamics stability of swimming in ostraciid fishes: role of the carapace in the smooth trunkfish *Lactophrys triqueter* (Teleostei: Ostraciidae) *J. Exp. Biol.* **206** 725–44
- Bartol I K, Gordon M S, Webb P, Weihs D and Gharib M 2008 Evidence of self-correcting spiral flows in swimming boxfishes *Bioinsp. Biomim.* **3** 014001
- Blake R W 1977 On ostraciiform locomotion *J. Mar. Biol. Assoc. UK* **57** 147–55
- Blake R W 1981 Mechanics of ostraciiform propulsion *Can. J. Zool.* **59** 1067–71
- Blake R W 1983 Swimming in the electric eels and knifefishes *Can. J. Zool.* **61** 1432–41
- Blake R W 2004 Fish functional design and swimming performance *J. Fish Biol.* **65** 1193–222
- Collins K, Forster F, Dolan S, Bowyer A and Megill W 2008 Kinematics and force characterization of a knifefish-inspired mechanical propulsor *Proc. Biological Approaches to Engineering* pp 30–3
- Deng X and Avadhanula S 2005 Biomimetic micro underwater vehicle with oscillating fin propulsion: system design and force measurement *Proc. 2005 IEEE Int. Conf. Robot. Auto. (Barcelona, Spain)* pp 3312–7
- Dollhopf S L, Ayala-Del-Río H L, Hashsham S A and Tiedje J M 2004 Multivariate statistical methods and artificial neural networks for analysis of microbial community molecular fingerprints *Molecular Microbial Ecology Manual* ed G A Kowalchuk, F J deBruijn, I M Head, A D Akkermans and J D van Elsas (Berlin: Springer) pp 1447–86
- Gordon M S, Hove J R, Webb P W and Weihs D 2000 Boxfishes as unusually well controlled autonomous underwater vehicles *Physiol. Biochem. Zool.* **73** 663–71
- Hove J R, O'Brien L M, Gordon M S, Webb P W and Weihs D 2001 Boxfishes (Teleostei: Ostraciidae) as a model system for fishes swimming with many fins: kinematics *J. Exp. Biol.* **204** 1459–71
- Kim E and Youm Y 2004 Design and dynamic analysis of fish robot: Potuna *Proc. IEEE Conf. Robot. Auto.* pp 4887–92
- Kong L X, Hodgson P D and Collinson D C 1998 Modelling the effect of carbon content on hot strength of steels using a modified artificial neural network *IJG Int.* **38** 1121–9
- Li J, Chan K H S, Kwok P Y L and Blake R W 2007 Evaluation using multilayer perception neural network: a case study of undulatory median fin swimming in the knifefish *Xenomystus nigri* *J. Fish Biol.* **71** 1203–7
- Lighthill M J 1969 Hydromechanics of aquatic propulsion: a survey *Ann. Rev. Fluid. Mech.* **1** 413–46
- Lighthill M J 1970 Aquatic animal propulsion of high hydromechanical efficiency *J. Fluid Mech.* **44** 265–301
- Masters T 1993 *Practical Neural Network Recipes in C++* (New York: Academic)
- McCulloch W S and Pitts W H 1943 A logical calculus of the ideas immanent in nervous activity *Bull. Math. Biophys.* **5** 115–33
- Morgansen K A, Duindam V, Mason R J, Burdick J W and Murray R M 2001 Nonlinear control methods for planar carangiform robot fish locomotion *Proc. IEEE Int. Conf. Robot. Auto* pp 427–34
- Ostrowski J and Burdick J 1998 The geometric mechanics of undulatory robotic locomotion *Int. J. Robot. Res.* **17** 683–701
- Salehfar H and Benson S A 1998 Electric utility coal quality analysis using artificial neural network techniques *Neurocomputing* **23** 195–206
- Trease B P, Lu K J and Kota S 2003 Biomimetic compliant system for smart actuator-driven aquatic propulsion: preliminary results *Proc. IMECE: ASME Int. Mech. Eng. Cong.* pp 1–10
- Triantafyllou M S and Triantafyllou G S 1995 An efficient swimming machine *Sci. Am.* **272** 64–70
- Triantafyllou M S, Triantafyllou G S and Yue D K P 2000 Hydrodynamics of fish-like swimming *Ann. Rev. Fluid Mech.* **32** 33–53
- Walker J A 2000 Does a rigid body limit maneuverability? *J. Exp. Biol.* **200** 1549–69